Dressing method of worm wheels for grinding face gears based on the principle of virtual phase transition

Guolong Li[1] · Ziyu Wang[1] · Kun He[2] · Zhishan Pu[1] · Bofeng Zhang[1]

Abstract
A method for dressing the worm wheel for grinding face gear with arbitrary modification amount by double cone dressing wheel is proposed. In order to ensure the machining accuracy and balance the machining time, the iteration method of tangent's deviation is proposed and the nominal residual mean error is defined. In order to improve the versatility of the scheme, a double cone dressing wheel and a universal worm grinding machine are used to carry out the research. Considering the complex space position transition, the principle of virtual phase transition is proposed to achieve the equivalent replacement of the motion of the double cone dressing wheel by the motion of the crown worm wheel, which consists of the principle of virtual tool setting and the principle of rotating virtual center distance. Finally, a simulation experiments is carried out on the dressing process of the modification crown worm wheel. The result shows that this method can effectively realize the modification dressing process of the crown worm wheel for grinding face gear.

Keywords Face gear · Modification · Crown worm wheel · Nominal residual mean error · Principle of virtual phase transition

1 Introduction

Face-gear has an irreplaceable position in the field of mechanical transmission, whose meshing state is shown in Fig. 1. Face-gear possesses the ability to transfer the equivalent energy in a larger space with less weight compared to traditional gear drives. Meanwhile, face-gear has the advantages of low requirements for axial positioning accuracy, large transmission ratio, large degree of overlap, stable working performance, and reliable load capacity. These characteristics allow face-gear to reduce load and thus concentrate energy, which is of great importance to the aviation sector where energy-efficient planning is significant.

Manufacturing of face gears has always been a research hotspot. Quite a few theories and researches on face gear

manufacturing have been proposed. Litvin et al. [1–3] led the development of face gears in the field of transmission, enriched the design theory of face gears, and perfected the structural design of reducers with face gears. Tang et al. [4, 5] developed a progressive grinding method and established a calculation method for the range of oscillation angles. Meanwhile, the mathematical model of the envelope of the worm wheel and face-gear were established. Zhou et al. [6] proposed a grinding method for manufacturing face gears with disk wheel, a computer-generated method for face gears by applying a conical spur involute shaper. Wang et al. [7] proposed an involute disc wheel which was used for grinding face gears.

Among the many methods for manufacturing face gears, worm wheel grinding has great advantages in the field of face-gear manufacturing as a highly efficient and precise method. Litvin et al. [8] proposed the worm wheel as the tool for grinding face gears firstly and also a design method for the worm wheel profile. Li et al. [9] proposed a dressing method of the crown worm wheel for grinding face gear on the common continuous generating gear grinding machine. He [10] re-planned the radial feed trajectory for the grinding face gear. Zhou et al. [11, 12] proposed a new geometric analysis of worm wheels and an efficient worm wheel dressing method with only one path.

✉ Guolong Li
glli@cqu.edu.cn

1   State Key Laboratory of Mechanical Transmission for Advanced Equipment, Chongqing University, Chongqing, China

2   Chongqing Key Laboratory of Manufacturing Equipment Mechanism Design and Control, Chongqing Technology and Business University, Chongqing, China
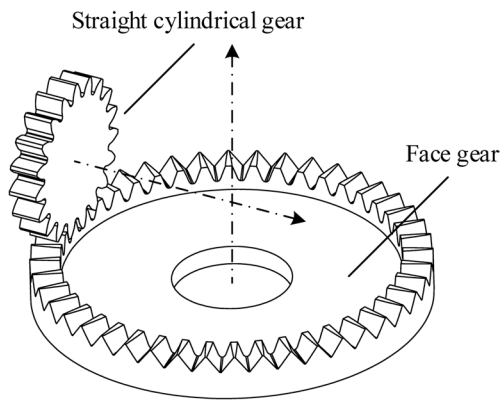
Fig. 1 Schematic diagram of face-gear drive

As the application range of face gears becomes wider and the manufacturing technology matures, face gear modification technology is gradually being paid attention to and researched. Tang et al. [13–15] have achieved important results in the in-depth study of the micro-creation mechanism using UVAG technology and have systematically analyzed the friction and abrasive wear of workpieces. Shi et al. [16] proposed a face gear modification method based on a new worm grinding method of face gears. Shen et al. [17] proposed a generic approach to design optimization techniques. Guo et al. [18] proposed an approximate definition method for grinding worm surfaces with variable meshing angles for grinding face gears. Peng and Zhou [19] proposed a surface activity modification (SAM) method to reduce vibration.

It can be seen that modification has a significant improvement on the meshing and dynamic performance of face gears. However, most of the current research has been on the modification-design. Modification-manufacturing is still lacking. Currently, commonly used forming dressing method is not general and universal when applied in the field of modification-manufacturing. The proposed modification method avoids the above problems well. However, it is required to solve complex systems of non-linear equations with complex initial value problems and singularity problems. Therefore, it is important to develop a modification method for dressing the crown worm wheel for grinding face-gear.

For the substitution of shapers with arbitrary modification-parameters in a universal worm grinding machine, this paper proposed a method for dressing the crown worm wheel for grinding face-gear with double cone dressing wheel. This paper analyzes the forming dressing process and its principles firstly. It will discuss the modification scheme with double cone dressing wheel and plan the machine motion path. Design the double cone dressing wheel profile and determine the range of tool parameters. A simulation experiment will

be conducted to verify the rationality of the program. This paper establishes an error prediction and evaluation model to balance machining cost and accuracy, completes the derivation of the relationship between the complex motion, and proposes a tool design method, thus constituting a complete set of dressing system.

2 Modification dressing principle of the crown worm wheel

Most of the existing crown worm wheels are dressed by using a forming dressing wheel to realize the profile complex by counter-rolling motion. Based on the meshing principle and surface envelope principle, the standard crown worm helical surface can be derived theoretically. On this basis, the dressing of the crown worm wheels can be realized by means of multi-axis linkage and trajectory planning of the machine. At the same time, changing the profile of the forming dressing wheel enables dressing of a modification crown worm wheel.

2.1 Forming principle of the crown worm wheel for grinding face gear

When calculating the crown worm helical surface, the traditional conjugate envelope surface method requires solving complex non-linear systems of equations, which cannot escape from complex initial value problems and singularity problems. According to the pre-research [9], the evolution calculation method of the crown worm for face gear grinding proposed is used. Imitating the evolution of rack shaper into ordinary cylindrical worm grinding wheel derived the formula of the evolution of the crown worm. The process will no longer be limited by initial values and singularities and has applicability and accuracy.

The profile line of standard shaper is standard involute, whose mathematical expression in the coordinate system of the shaper is

$$\vec{r_s}(\theta_s) = \begin{bmatrix} \pm \text{rbs} \times [\sin(\theta_s + \theta_{os}) - \theta_s \times \cos(\theta_s + \theta_{os})] \\ \text{rbs} \times [\cos(\theta_s + \theta_{os}) + \theta_s \times \sin(\theta_s + \theta_{os})] \\ 0 \\ 1 \end{bmatrix}$$

(1)

where *rbs* is the involute base circle radius; θ_s is the involute spreading angle; θ_{os} is the involute spreading angle at addendum; "+" corresponds to the right side of the tooth surface; and "−" corresponds to the left side of the tooth surface.

The shaper profile with modification-parameters is established, as shown in Fig. 2. To ensure that the addition of the modification-parameters does not affect the diameter of the double cone dressing wheel, the modification-parameters are
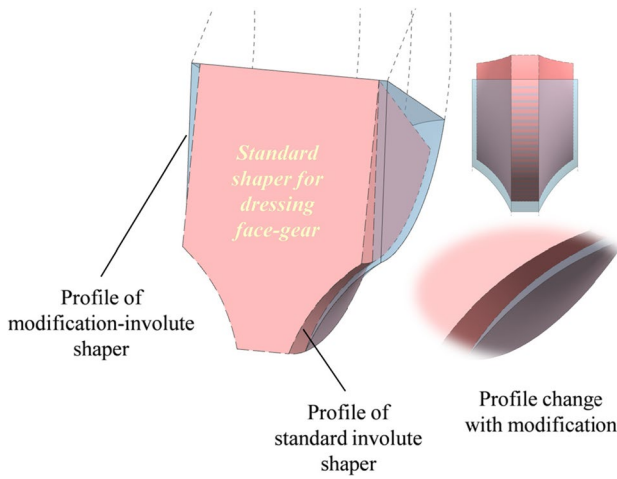
Fig. 2 Schematic diagram of the profile of the modification shaper

Fig. 3 The coordinate systems for the shaper and the crown worm

superimposed on the horizontal axis of the standard involute in the form of a trim modification-curve. Meanwhile, in order to achieve the purpose of higher-order arbitrary modification, the modification-curve is set to three terms, which are associated with the 0th, 1st, and 2nd order terms of the involute spreading angle, thus respectively characterizing the translation in the X-direction, tangential rotation, and curvature variation. Therefore, the involute equation with modification-parameters is expressed as follows

$$x = \text{rbs} \times \left[\sin\left(\theta_s + \theta_{os}\right) - \theta_s \times \cos\left(\theta_s + \theta_{os}\right) \right] + \left(ax \times \theta_s^2 + bx \times \theta_s + cx\right) \tag{2}$$

$$y = \text{rbs} \times \left[\cos\left(\theta_s + \theta_{os}\right) + \theta_s \times \sin\left(\theta_s + \theta_{os}\right) \right] \tag{3}$$

where *rbs* is the involute base circle radius; θ_s is the involute spreading angle; θ_{os} is the involute spreading angle at addendum; and *ax*, *bx*, and *cx* is the modification-parameters.

The relationship between the coordinate system of the shaper and the coordinate system of the crown worm wheel is established, as shown in Fig. 3. $O_w - X_w Y_w Z_w$ is the dynamic coordinate system fixed with the crown worm
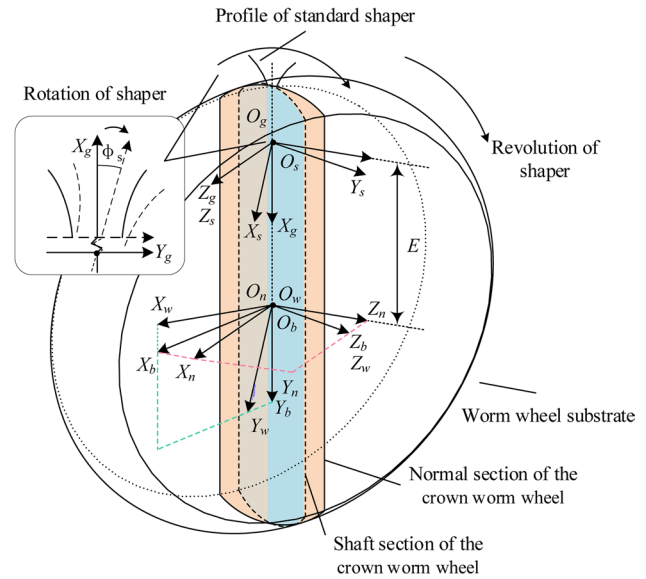
wheel; $O_b - X_b Y_b Z_b$ is the fixed coordinate system; and the plane $Y_b O_b Z_b$ coincides with the worm shaft section. $O_n - X_n Y_n Z_n$ is the fixed coordinate system, and the plane $Y_n O_n Z_n$ coincides with the worm normal section. $O_s - X_s Y_s Z_s$ is the dynamic coordinate system fixed with the standard shaper profile. $O_g - X_g Y_g Z_g$ is the fixed coordinate system of the shaper.

According to the principle of evolutionary calculation, the crown worm's helical surface can be regarded as the involutes sweeping along the crown worm surface, respectively. According to the principle of motion decomposition, this motion can be decomposed into the rotation of the involutes around the axis of the shaper and the rotation of the involutes around the axis of the crown worm, which are carried out simultaneously according to a certain speed ratio. It is almost like the rotation and revolution of the earth. From this, the coordinate transformation matrix from the shaper coordinate system $O_g - X_g Y_g Z_g$ to the worm wheel surface coordinate system $O_w - X_w Y_w Z_w$ is obtained as

$$M_{wg} = \begin{bmatrix} \cos\varphi_s \sin\left(\frac{\varphi_S}{NS}\right) \sin\lambda - \cos\left(\frac{\varphi_S}{NS}\right) \sin\varphi_s & -\sin\left(\frac{\varphi_S}{NS}\right) \sin\varphi_s - \cos\left(\frac{\varphi_S}{NS}\right) \cos\varphi_s \sin\lambda & \cos\varphi_s \cos\lambda & E\sin\varphi_s \\ \cos\left(\frac{\varphi_S}{NS}\right) \cos\varphi_s + \sin\left(\frac{\varphi_S}{NS}\right) \sin\varphi_s \sin\lambda & \cos\varphi_s \sin\left(\frac{\varphi_S}{NS}\right) - \cos\left(\frac{\varphi_S}{NS}\right) \sin\varphi_s \sin\lambda & \cos\lambda \sin\varphi_s & -E\cos\varphi_s \\ -\cos\lambda \sin\left(\frac{\varphi_S}{NS}\right) & \cos\left(\frac{\varphi_S}{NS}\right) \cos\lambda & \sin\lambda & 0 \\ 0 & 0 & 0 & 1 \end{bmatrix} \tag{4}$$

where *NS* is the number of teeth of shaper; λ is the spiral angle; E is the center distance between face gear and shaper; and φ_s is the rotation angle of the shaper.

Then, according to the principle of coordinate transformation, the final calculation of the equation of the modification crown worm helical surface is
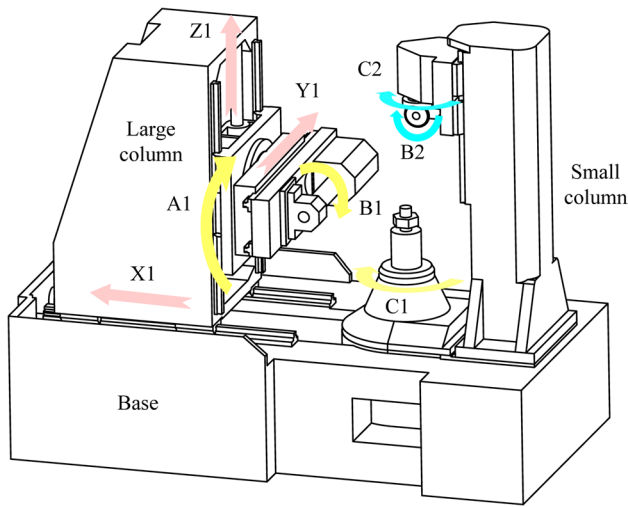
Fig. 4 Schematic diagram of the structure of worm grinding machine

In the forming dressing process, the $B1$-axis is usually used as the worm wheel rotation axis and the $B2$-axis as the dressing wheel rotation axis. According to the principle of evolution calculation, the forming dressing wheel needs to sweep along the surface of the worm wheel to form a helical trajectory. The dressing wheel only self-rotates at high speed during dressing. Four-axis linkage of $A1$, $B1$, $Y1$, and $Z1$ axes control the worm wheel position. $A1$ and $B1$ axes rotate in a ratio relationship to complete the spiral line. $Y1$ and $Z1$ axes are used as compensating axes to eliminate the influence of machine parameters.

Based on the above process and structural features of the machine topology chain, the universal worm grinding machine shows the following characteristics in grinding the crown worm wheel for grinding face gear:

$$\overrightarrow{r_{wg}} = \begin{bmatrix} x_{wg} \\ y_{wg} \\ z_{wg} \\ 1 \end{bmatrix} = \begin{bmatrix} \begin{aligned} & E\sin(\varphi_s) - (\cos(\varphi_s/N_s)\sin(\varphi_s) - \cos(\varphi_s)\sin(\lambda)\sin(\varphi_s/N_s))(cx + bx \times \theta_s + r_{bs}(\cos(\theta_s + \theta_{os}) \\ & + \theta_s\sin(\theta_s + \theta_{os}) + ax \times \theta_s^2) - r_{bs}(\sin(\varphi_s)\sin(\varphi_s/N_s) + \cos(\varphi_s)\cos(\varphi_s/N_s)\sin(\lambda)) \\ & \times(\sin(\theta_s + \theta_{os}) - \theta_s\cos(\theta_s + \theta_{os})) \end{aligned} \\ \\ \begin{aligned} & (\cos(\varphi_s)\cos(\varphi_s/N_s) + \sin(\varphi_s)\sin(\lambda)\sin(\varphi_s/N_s))(cx + bx \times \theta_s + r_{bs}(\cos(\theta_s + \theta_{os}) \\ & + \theta_s\sin(\theta_s + \theta_{os}) + ax \times \theta_s^2) - E\cos(\varphi_s) + r_{bs}(\cos(\varphi_s)\sin(\varphi_s/N_s) - \cos(\varphi_s)\sin(\lambda)\sin(\varphi_s/N_s)) \\ & \times(\sin(\theta_s + \theta_{os}) - \theta_s\cos(\theta_s + \theta_{os})) \end{aligned} \\ \\ \begin{aligned} & r_{bs}\cos(\lambda)\cos(\varphi_s/N_s)(\sin(\theta_s + \theta_{os}) - \theta_s\cos(\theta_s + \theta_{os})) - \cos(\lambda)\sin(\varphi_s/N_s) \\ & \times(cx + bx \times \theta_s + r_{bs}(\cos(\theta_s + \theta_{os}) - \theta_s\sin(\theta_s + \theta_{os})) \\ & + \theta_s\sin(\theta_s + \theta_{os})) + ax \times \theta_s^2 \end{aligned} \\ \\ 1 \end{bmatrix} \tag{5}$$

2.2 Forming dressing method of the crown worm wheel for grinding face gear

The structure of the universal worm grinding machine is shown in Fig. 4. There are two topology chains for universal worm gear grinding machine, "*Base–X1–Z1–A1–Y1*" and "*Base–C2–B2*", respectively. $X1$, $Z1$, $A1$, $Y1$, $B1$, and $C2$ axes form a six-axis linkage relationship. While dressing the crown worm wheel, the X-axis controls the feed distance of the worm wheel; the Z-axis controls the feed depth of the worm wheel; the A-axis controls the rotation angle of the worm wheel; the Y-axis controls the axial feed movement of the worm wheel; the $B1$-axis controls the rotation speed of the worm wheel; the $B2$-axis controls the rotation speed of the shaper; and and the $C2$-axis controls the nominal screw lead angle.

- The Y-axis direction is influenced by the A-axis rotation angle in the machine coordinate system. This is caused by the fact that the A-axis is at a higher level than the Y-axis in the topology chain.
- The double cone dressing wheel cannot rotate around the A-axis direction. There is no special dressing wheel rotation mechanism in the universal worm grinding machine.
- During the dressing process the geometric center of the double cone dressing wheel cannot change its absolute coordinates in the machine coordinate system, which depends on the machine structure parameters and is not affected by the motion of each axis.
- The distance between the center of the dressing wheel and the center of rotation of the A-axis on the horizontal axis depends on the structural parameters of the machine and is a fixed value.

3 Modification method of the crown worm wheel with double cone dressing wheel

To dress a modification crown worm wheel using the above method, it is required to change the profile of the forming dressing wheel to correspond. But that means that different forming dressing wheels are needed for dressing the crown worm wheels with different modification parameters, which is not universally applicable. Therefore, the universal double cone dressing wheel is selected as the dressing tool for the crown worm wheel. Dress the crown worm wheel with straight cutting edge in place of forming roll by tangential approximation.

3.1 Determination of the scheme for dressing the crown worm wheel for grinding face gear

3.1.1 Tangent approximation of involute with arbitrary modification-parameters

The profile of double cone dressing wheel and its basic parameters are shown in Fig. 5. The double cone dressing wheel consists of working interval and extension substrate. The working interval is composed of tapered linear segments rotating along the axis of the double cone dressing wheel. The intersection angle of the extension lines of the left and right cutting edges on the shaft section of the double cone dressing wheel axis is the cone-apex angle.

Formed involute dressing wheels only rotate rapidly about their own axes during dressing of the crown worm. The process can be regarded as that the forming wheel sweeps along the spiral line on the matrix of the worm wheel to form the crown worm helical surface. Therefore, the intersection line between the worm wheel and the dressing wheel shaft section is the same as the dressing wheel profile. Approximation of the outline can be achieved by grinding multiple times by changing the position and attitude of double cone dressing wheel. The principle is that the linear cutting edge of the double cone dressing wheel coincides with the tangent of the modification involute, as shown in Fig. 6. By using a different tangent line as the starting position of the double cone dressing wheel, the modification worm gear grinding profile can be enveloped by sweeping along the spiral line several times, thus enabling the dressing of the crown worm wheel for grinding face gear with an arbitrary modification-parameters.

3.1.2 Calculate the times of dressing by the iteration method of tangent's deviation

Inevitably, the tangent approximation to the modification-involute will introduce deviations. Theoretically, the deviation is 0 when the times of dressing are infinite, and the deviation is larger when the times of dressing are smaller. However, in engineering, the increase in the time of dressing also means an increase in processing time and processing cost. Therefore, finding the balance between machining accuracy and machining time can make the machining solution more reasonable.

The nominal residual mean error is used as a measure of machining accuracy, and the iteration method of tangent's deviation is used to control the nominal residual mean error to achieve the target nominal residual mean error and minimize the number of dressing times, calculate the recommended times of dressing, and determine the dressing scheme. The principle of the iteration method of tangent's deviation is shown in Fig. 7, where A and B are the dressing contact points. Make the involute tangent line through the contact point respectively, and the expression for the slope of the tangent line at the tangent point of the modification-involute is calculated as follows

$$k = \frac{\left(rbs \times \theta_s \times \cos\left(\theta_s + \theta_{os}\right)\right)}{bx + 2 \times ax \times \theta_s + rbs \times \theta_s \times \sin\left(\theta_s + \theta_{os}\right)} \tag{6}$$

The tangents at points A and B intersect at point G. Take the nearest point H on the involute from point G as the corresponding point and take the projection of this distance on the normal vector at H as the nominal residual error δ. Considering the influence of the radius of curvature of the modification-involute on the equipartition density, the involute spread angle θ_s used as the basic scale to equipartition the modification-involute. The average of all the above projections is calculated as the nominal residual mean error according to the different number of equipartition. The minimum times of dressing whose nominal residual error is less than the target nominal residual error are sought as the recommended times of dressing by mathematical iteration. Record the coordinates of the tangent point and the slope of its corresponding tangent line. Determine the initial position of the double cone dressing wheel by the tangent point coordinates and determine the initial attitude of the double cone dressing wheel by the slope.

3.2 The principle of virtual phase transition

The relative positions of the crown worm wheel and the double cone dressing wheel are not the same for different dressing times when using tangent to approach the modification forming roll contour. As shown in Fig. 6, the change in position of the tangent point of the modification-involute leads a change in the center of the double cone dressing wheel and the different slopes at different tangent points of the modification-involute lead a change in the angles of the
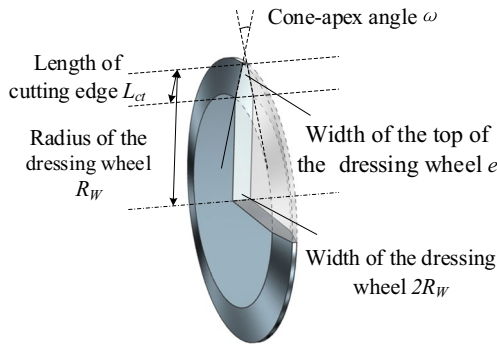
Fig. 5 Schematic diagram of the double cone dressing wheel

Fig. 6 Schematic diagram of the tangent approximation of modification involute

double cone dressing wheel axis. That means the angle of deflection and the center position of the dressing wheel need to be varied in different dressing times. However, according to the motion characteristics analyzed in the previous section, the double cone dressing wheel cannot rotate around the A-axis direction and the geometric center cannot be changed. Therefore, it is necessary to plan the grinding path to achieve equivalent substitution.

Divide the motion of double cone dressing wheel into translation and rotation. In this paper, the principle of virtual tool setting is proposed to achieve the equivalent replacement of the dressing wheel translation motion, and the principle of rotating virtual center distance is proposed to achieve the equivalent replacement of the dressing wheel rotation motion. Specific programs will be discussed in detail below.

3.2.1 Determination of dressing start point based on the principle of virtual tool setting

The principle of virtual tool setting is proposed to achieve the equivalent replacement of the dressing wheel translation motion. The principle of virtual tool setting is shown in Fig. 8, where the cutting edge of the double cone dressing wheel is coincident with the tangent line over the tangent point. Point Q is a tangent point on the profile of the virtual dressing wheel, which is also a dressing point for the current machining. ε is the angle between the axis of the double cone dressing wheel and the axis of the virtual dressing wheel at this time, called the virtual angle of double cone dressing wheel rotation.

The state in which the center of the double cone dressing wheel is aligned with the center of the crown worm wheel, and the surfaces are in perfect contact is regarded as the tool setting state. In this state, the center of the worm wheel is named as the actual tool setting point of the worm wheel, and it is also used as the starting point of the dressing process. So as shown in Fig. 8, O_W is the actual tool setting point of the worm wheel. The coordinates of this point are
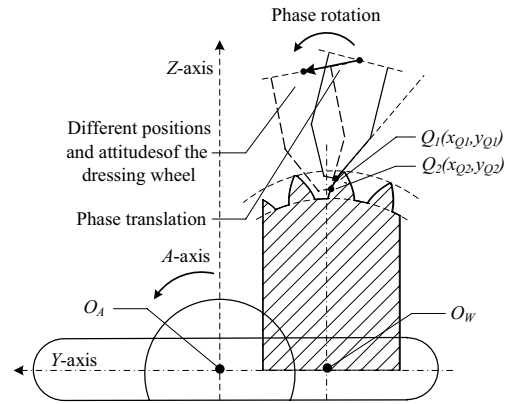
only determined by the machine tool parameters, the dressing wheel radius, and the worm wheel radius. Name the center of the dressing wheel in this state as the actual tool setting point of the dressing wheel.

However, the tool setting status of the virtual forming wheel is not the same as the actual tool setting status. According to the definition of the tool setting state above, the virtual tool setting state is when the center of the virtual forming wheel is aligned with the center of the crown worm wheel, and the surfaces are in perfect contact. Therefore, when the center line of the virtual shaper's shaft section coincides with the center line of the double cone dressing wheel's shaft section, and the top of the two coincide, the center position of the double cone dressing wheel is the virtual tool setting point of the double cone dressing wheel, as shown in point O_B in Fig. 8.

The actual tool setting point and the virtual tool setting point of the double cone dressing wheel form the vector $\overrightarrow{O_A O_B}$, which is the target compensation vector. In the case where only translation is considered, the compensation vector of the crown worm wheel is parallel to $\overrightarrow{O_A O_B}$. Decompose the vector $\overrightarrow{O_A O_B}$ into the Y-axis and Z-axis of the machine to obtain the worm wheel compensation path.

Based on the above theory and the principle of virtual tool setting, the crown worm wheel should be moved to the virtual tool setting position as the starting point before the dressing process and after the tool setting process is completed. The travels of the $Y1$ and $Z1$ axes are recorded as Y_p and Z_p, whose specific expressions in different dressing are as follows

$$Y_p = \sqrt{\left[y_Q - y_0 + R_w \times (\cos\varepsilon - 1)\right]^2 + \left[x_Q - R_w \times \sin\varepsilon\right]^2} \times \cos\eta \tag{7}$$

$$Z_p = \sqrt{\left[y_Q - y_0 + R_w \times (\cos\varepsilon - 1)\right]^2 + \left[x_Q - R_w \times \sin\varepsilon\right]^2} \times \sin\eta \tag{8}$$
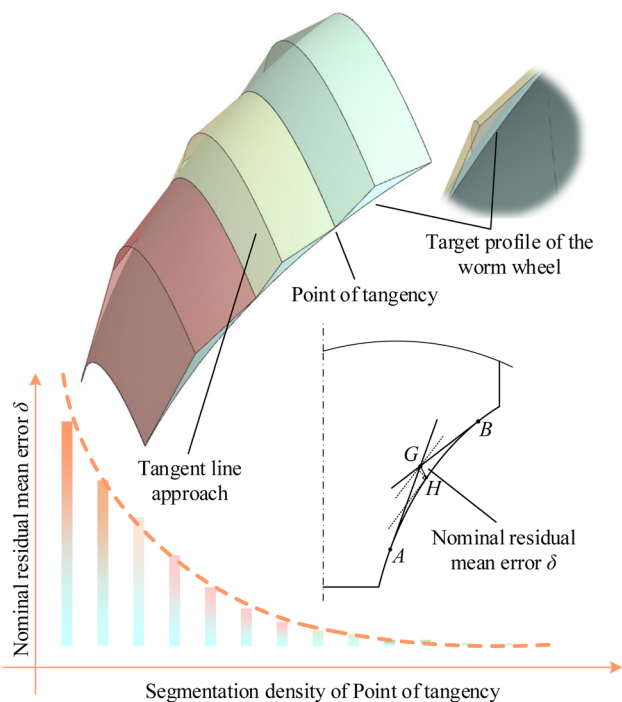
Fig. 7 Schematic diagram of the iteration method of tangent's deviation

Fig. 8 Schematic diagram of the principle of virtual tool setting

$$\eta = \tan^{-1}\left(\frac{y_Q - y_0 + R_w \times (\cos\varepsilon - 1)}{x_Q - R_w \times \sin\varepsilon}\right) - \varepsilon \tag{9}$$

$$\varepsilon = \tan^{-1}(K_Q) - \gamma \tag{10}$$

where, R_w is the radius of double cone dressing wheel; y_Q is the longitudinal coordinate of the tangent point; y_0 is the longitudinal coordinate of the starting point of the involute; x_Q is the horizontal coordinate of the tangent point; ε is the virtual rotation angle of the dressing wheel; γ is the cone-apex angle of the dressing wheel; K_Q is the slope of the tangent line at the tangent point.

At the same time, the machine fixed parameter e_y, which is the offset between the center of rotation of $A1$-axis and the center of dressing wheel in horizontal direction should also be considered as changed. The magnitude of the change Δe_y is equal to Y_p. It is important to note that when the value of ε is negative, the values of Y_p and Z_p should be calculated as the opposite.

3.2.2 Machine tool motion design based on the principle of rotating virtual center distance

The principle of rotating virtual center distance is proposed to achieve the equivalent replacement of the dressing wheel rotation motion. The principle of rotating virtual center
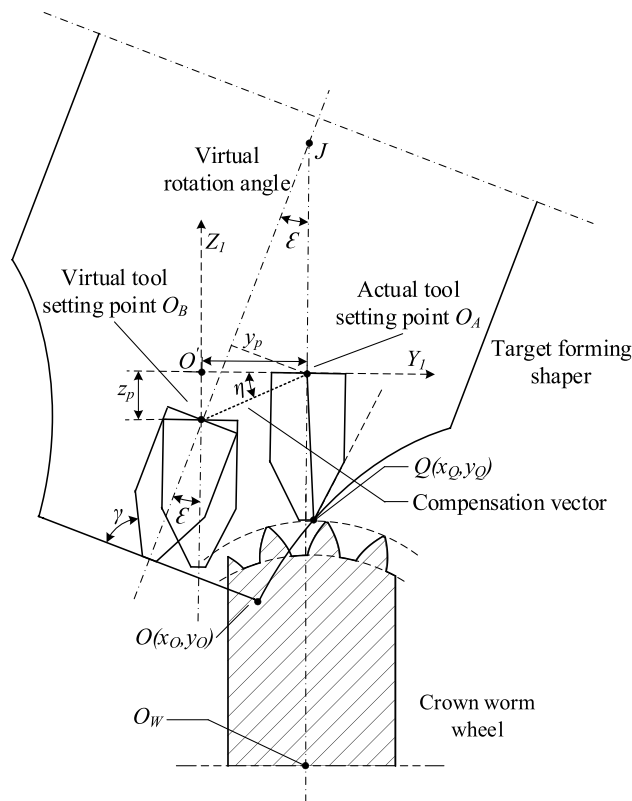
distance is shown in Fig. 9. Considering that the double cone dressing wheel in the universal worm grinding machine cannot rotate around the direction of A-axis, and meanwhile there is a distance between the center of the shaper and the center of rotation of A-axis on the horizontal coordinate axis, the relative positions of the crown worm wheel and the double cone dressing wheel are shown in Fig. 9a. Here O_A is the center of rotation of the A-axis; O_W is the center of the crown worm wheel, and O_G is the center of the double cone dressing wheel. The axis of the double cone dressing wheel is actually parallel to the axis of the worm wheel. So the virtual angle of the double cone dressing wheel ε is formed by the axis of the hypothetical rotated dressing wheel and the axis of the actual dressing wheel. Then, the position relationship between the actual machining state and the theoretical machining state can be obtained by rotating the overall position ε around the center O_G oppositely, as shown in Fig. 9b. Here, O'_A is the theoretical A-axis rotation center; O'_W is the theoretical crown worm wheel center; O'_S is the theoretical virtual shaper center.

Specific analysis of the four-axis linkage travel with $A1$, $B1$, $Y1$, and $Z1$ axes is shown in Fig. 9c. Firstly, find the theoretical processing state at any moment. The theoretical machining state of crown worm wheel consists of the wheel position and the wheel attitude. The position of the

worm wheel is determined by the center of the wheel, and the attitude of the worm wheel is determined by the angle of rotation of the wheel. Assuming that the angle of rotation of $B1$-axis at a given moment is B_i relative to the initial moment, the target rotation of $A1$-axis can be determined from the transmission ratio

$$A_i = B_i/Z_s \tag{11}$$

where A_i is the target rotation of $A1$-axis; Z_s is the number of teeth of the virtual shaper.

Then, the center of the crown worm wheel at this moment is H, where O'_W reaches after rotating A_i around point O'_S. This point is the theoretical crown worm wheel center. $\overline{O'_S H}$ is the theoretical crown worm wheel centerline.

Determine the actual processing status on this basis. To ensure the correct attitude of the crown worm wheel, the actual worm wheel centerline should be parallel to the theoretical worm wheel centerline. Therefore, the actual A-axis rotation angle at any moment should be

$$\Delta A_i = A_i - \varepsilon \tag{12}$$

Also, to ensure the correct position of the crown worm wheel, the actual worm wheel center and the theoretical worm wheel center should coincide. Therefore, $\overline{O_A H}$ is the compensation vector. Decompose this compensation vector to the $Y1$ and $Z1$ axes of the machine, and its decomposition corresponds to the compensation travels of the $Y1$ and $Z1$ axes, Dy_i and Dz_i, respectively. Note that at this time the $Y1$-axis direction is affected by the $A1$-axis rotation angle. Finally, it is concluded that the travels of the $Y1$ and $Z1$ axes at any time are

$$Dy_i = \frac{\left[(E + l) \times \sin \varepsilon - E \times \sin A_i \times \cos \left(\varepsilon - \frac{A_i}{2}\right)/\sin \left(\frac{\pi}{2} - \frac{A_i}{2}\right) - e_y\right]}{\cos (A_i - \varepsilon)} + e_y \tag{13}$$

$$Dz_i = -\left[(E + l) \times \sin \varepsilon - E \times \sin A_i \times \cos \left(\varepsilon - \frac{A_i}{2}\right)/\sin \left(\frac{\pi}{2} - \frac{A_i}{2}\right) - e_y\right] \times \tan (A_i - \varepsilon)$$
$$+ (E + l) \times (1 - \cos \varepsilon) - E \times \cos (A_i - \varepsilon) + E \times \cos \varepsilon \tag{14}$$

where E is the axis distance between the crown worm wheel and the virtual shaper; l is the distance from the center of the virtual shaper to the center of the dressing wheel; e_y is the offset between the center of rotation of $A1$-axis and the center of dressing wheel in horizontal direction.

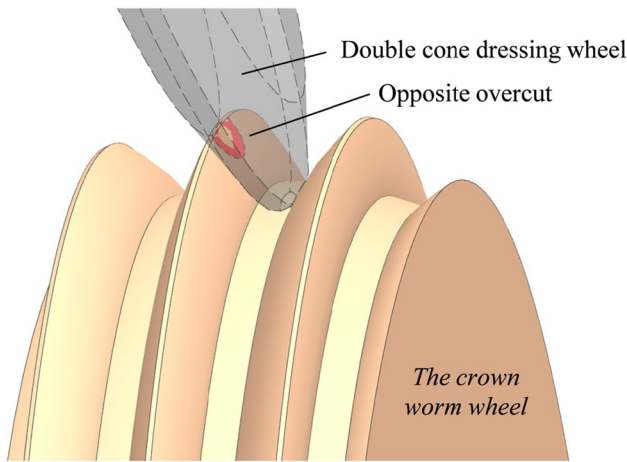**Fig. 9** Schematic diagram of the principle of rotating virtual center distance
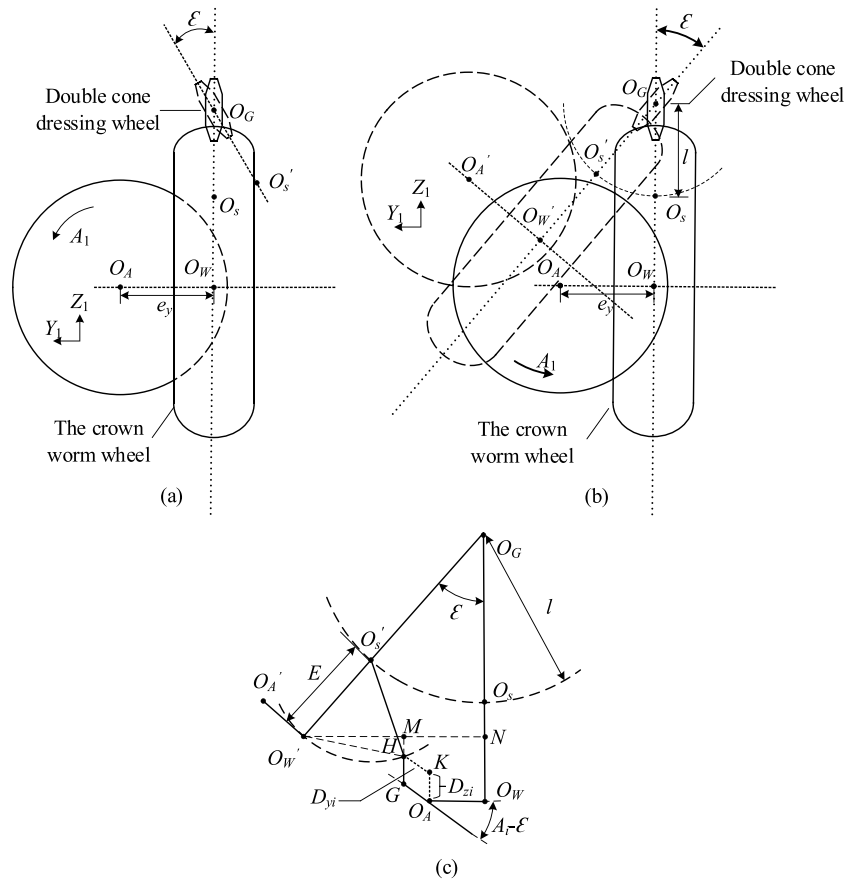
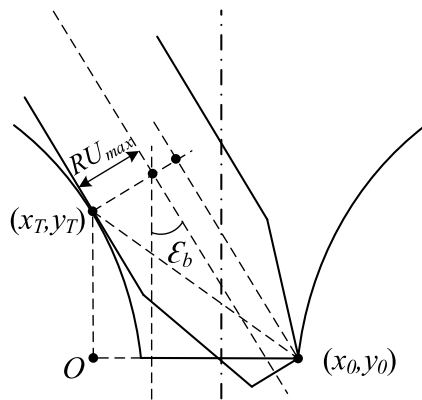Fig. 10 Schematic diagram of the opposite overcut

Fig. 12 Minimum cutting edge length

Fig. 11 Maximum dressing wheel half-width

Fig. 13 Range of cone-apex angle

4 Parameter design of the double cone dressing wheel

Optimize tool parameter design for the above dressing process. Propose guidelines for the design of double cone dressing wheel, which aims to enhance process operability and engineering practicality.

4.1 Maximum dressing wheel half-width

The tool design solution is proposed for the overcutting phenomenon that may arise from the above process method,
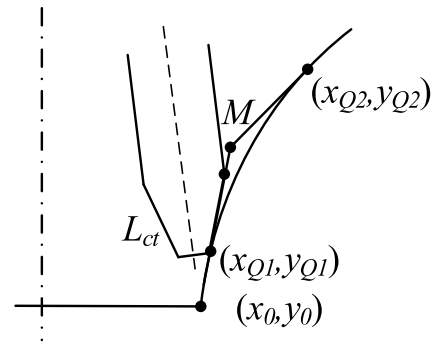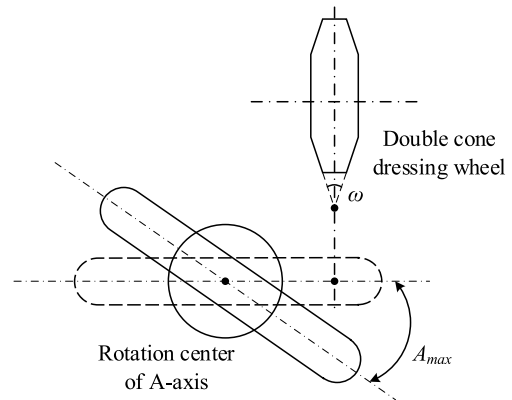
as shown in Fig. 10. When the dressing wheel half-width *RU* is too large, there will be interference on the opposite side when the double cone dressing wheel grinds the bottom of the crown worm wheel, and such interference is called opposite overcut.

Take the right crown worm helical surface as an example to analyze the critical conditions of its appearance, as shown in Fig. 11. The tangent line of the crown worm left helical surface at the *T* point is parallel to the center line of the double cone dressing wheel when dressing the bottom of the worm wheel.

According to the geometric relationship, the maximum dressing wheel half-width RU_{MAX} is

Table 3 Calculation of virtual tool setting parameters on the left helical surface

	1L	2L	3L	4L	5L	6L	7L	8L	9L	10L
ε	−17.2572	−15.3770	−12.6460	−9.6125	−6.4378	−3.1865	0.1107	3.4373	6.7836	10.1437
Y_p	19.1323	16.7547	13.2839	9.3699	5.2186	0.9263	−3.4487	−7.8637	−12.2842	−16.6797
Z_p	−2.6436	−2.3359	−2.0309	−1.9723	−2.2397	−2.8676	−3.8734	−5.2659	−7.0495	−9.2253

Table 1 Basic parameter values

Design parameters	Value
Number of teeth of shaper n_s	23
Number of teeth of face gear n_2	48
Number of worm n_w	1
Modulus m/mm	3.9
Pressure angle α/°	25
Tooth height coefficient h_a^*	1
Bottom clearance coefficient c^*	0.25
Dressing wheel radius R_w/mm	70
Cone-apex angle of double cone dressing wheel γ/°	60
Nominal residual mean error δ/mm	0.01

$$RU_{MAX} = \sqrt{(x_T - x_0)^2 + (y_T - y_0)^2} \times \sin\left(\frac{\pi}{2} - |\varepsilon_b| - \arctan\left(\left|\frac{(y_T - y_0)}{(x_T - x_0)}\right|\right)\right) - \frac{e}{2}$$

(15)

where x_T and y_T and the left tangent point's horizontal and vertical coordinates; ε_b is the value of ε at the start point of the right involute; e is the width of the top of the double cone dressing wheel.

4.2 Minimum cutting-edge length

The tool design solution is proposed for the residual phenomena that may arise from the above process methods, as shown in Fig. 12. Surface residue occurs when the cutting-edge of double cone dressing wheel is too short.

To avoid this phenomenon, the minimum cutting-edge length of the double cone dressing wheel should meet

$$L_{ct\,min} = \max\left(L_q\right)$$

(16)

where L_q is the length of all tangent segments. All tangent lengths are computed by the iteration method of tangent's deviation given in Section 3.1.

4.3 Range of cone-apex angle

The tool design solution is proposed for the overswing phenomenon of $A1$-axis that may arise from the above process methods, as shown in Fig. 13. When the double cone dressing wheel's cone-apex angle is in a certain range, over travel phenomenon of $A1$-axis will appear.

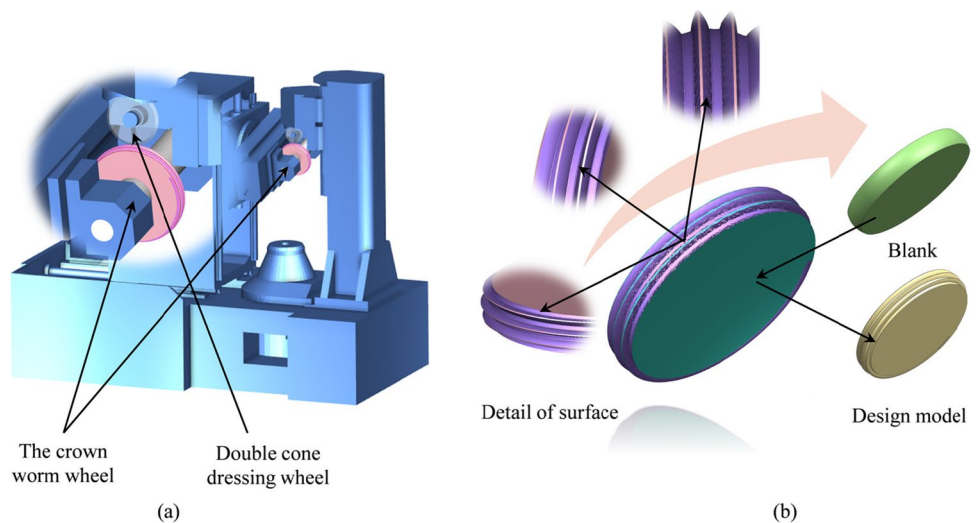To avoid this phenomenon, the double cone dressing wheel's cone-apex angle should satisfy the inequality

$$\left|\arctan\left(K_Q\right) - (2\pi - \omega)/2\right|_{\max} \leq A_{\max} - S \times \pi/N_s$$

(17)

where K_Q is the slope of tangent line; $A_{\max}$ is the maximum rotation angle of $A1$-axis of worm grinding machine; S is the nominal overlap which usually takes the value of 2; N_s is the number of teeth of shaper.

Table 2 Calculation of virtual tool setting parameters on the right helical surface

	1R	2R	3R	4R	5R	6R	7R	8R	9R	10R
ε	17.2572	15.3770	12.6460	9.6125	6.4378	3.1865	−0.1107	−3.4373	−6.7836	−10.1437
Y_p	−19.1323	−16.7547	−13.2839	−9.3699	−5.2186	−0.9263	3.4487	7.8637	12.2842	16.6797
Z_p	−2.6436	−2.3359	−2.0309	−1.9723	−2.2397	−2.8676	−3.8734	−5.2659	−7.0495	−9.2253

Fig. 14 Simulation process and simulation results schematic

The crown worm wheel

Double cone dressing wheel

(a)

Blank

Detail of surface

Design model

(b)

Overcut		Residual	
Range	Color	Range	Color
1.00000	Red	1.00000	Blue
0.50000	AutoDiff-G5	0.50000	Machine-15
0.20000	AutoDiff-G5	0.20000	Machine-14
0.10000	AutoDiff-G5	0.10000	Machine-13
0.01000	AutoDiff-G5	0.01000	Machine-12
0.00100	AutoDiff-G5	0.00100	Machine-11
0.00000	Light Sea Green	0.00000	Light Sea Green

Element:gear1	Minimum deviation					Minimum deviation				
	No.	Dev.	X	Y	Z	No.	Dev.	X	Y	Z
	41	0	99.1317	-1.2319	12.53	146	-0.0032	90.9596	-3.5954	17.5791

Fig. 15 Machining accuracy measurement and error visualization

5 Simulation experiment of dressing the modification crown worm wheel

VERICUT is used to simulate the dressing process of the modification crown worm wheel to verify the correctness of the method. VERICUT is a specialized CNC machining simulation software. It has a complete and realistic simulation operation process, provides high-precision calculation results, and provides a simulation experiment platform for professional CNC machine technicians. It is often used to verify the machining process and predict the machining experiment results. The adopted face gear parameters and double cone dressing wheel parameters are shown in Table 1:

According to the technical route described above, the iteration method of tangent's deviation is used to control the nominal residual mean error, calculate the recommended number of dressing, and determine the dressing scheme. Take the modification-parameter ax = 0.25, bx = 0.3 and cx = 0.1 in this case. Set the target nominal residual mean error to 0.01 mm. The value of S returned by iterative computation is 9, so the recommended number of dressing is 10. The returned nominal residual mean error at this point is 0.0087, which is smaller than the target nominal residual mean error. Thus, record the coordinates of the tangent point and the slope of its corresponding tangent line equation.

Based on the principle of virtual tool setting, the crown worm wheel should be moved to the virtual tool setting position as the starting point before dressing process and after the tool setting process is completed. At the same time, the machine fixed parameter e_y, which is the offset between the center of rotation of A1-axis and the center of dressing wheel in horizontal direction should also be considered as changed.

According to the formula in Section 2.2, the starting point and the change of machine parameters are calculated as, shown in Table 2 and 3, respectively:

Based on the principle of rotating virtual center distance, replace the rotation of the double cone dressing wheel along the A-axis direction with the machine tool four-axis linkage equivalently. Calculate the discrete point coordinates of the spline according to the formula in Section 2.3. Calculate process start point offset in combination with the principle of virtual tool setting and write complete NC programs.

Load NC program into VERICUT and build the worm grinding machine model. Siemens 840D CNC is selected to configure the machining simulation environment. The simulation process and results of the dressing process are shown in Fig. 14a.

Details of the workpiece are shown in Fig. 14b. It can be seen that the overall shape of the crown worm wheel is complete. Double helix surface is fully enveloped. The results are consistent with the design model expectations, preliminary verification of processing process feasibility.

The simulation accuracy is measured using VERICUT to compare the design model and the machined workpiece, as shown in Fig. 15. The results show that there is a residual of less than 0.01 mm in the middle of the crown worm helical surface, which is the principal deviation caused by the process scheme. It is consistent with the experimental expectation and proves the correctness of the iteration method of tangent's deviation. And there is a phenomenon of overcutting not more than 0.01 mm at the bottom of the crown worm wheel. This is because the width of the top of the double cone dressing wheel is not 0. Interference occurs at the bottom surface of the worm wheel when dressing the

position of the starting point. However, this surface is not the working surface and does not participate in the rolling motion with the face gear. Therefore, this is an acceptable error. The deviation of the remaining positions is less than 0.005 mm, which proves the feasibility and completeness of this dressing solution with double cone dressing wheel.

6 Conclusions

A complete modification method for dressing the crown worm wheel is proposed, and the machining tool parameters are studied, where double cone dressing wheels can be used for grinding the crown worm wheels with any modification-parameters. This method does not require solving any complex system of nonlinear equations. Simulation experiment with VERICUT shows the correctness of the proposed method. Based on the above research, the following conclusions were drawn:

- The use of double cone dressing wheel and universal worm grinding machine as the machining tool for this study improves the universality of the solution. It realizes equivalent substitution of involute forming wheel with arbitrary modification-parameters, which is flexible and practical.
- The error calculation model and the iterative calculation method are established. The proposed iteration method of tangent's deviation can effectively ensure machining accuracy while reducing grinding time, lowering machining costs, and improving machining efficiency.
- The principle of virtual phase transition is proposed to calculate the machine motion trajectories. It realizes equivalent substitution of translational and rotational movements of the dressing wheel. Complete envelope of the crown worm helical surface can be accomplished by dressing pre-processing and sample point calculation.

Declarations

Ethics approval Not applicable.

Consent to participate Not applicable.

Consent for publication Yes.

Competing interests The authors declare no competing interests.

References

1. Litvin FL, Egelja A, Tan J, Heath G (1998) Computerized design, generation and simulation of meshing of orthogonal offset face-gear drive with a spur involute pinion with localized bearing contact. Mech Mach Theory 33:87–102. https://doi.org/10.1016/S0094-114X(97)00022-0
2. Litvin F, Wang J, Bossler R et al (1994) Application of face-gear drives in helicopter transmissions. J Mech Des 116:672–676. https://doi.org/10.1115/1.2919434
3. Litvin FL, Zhang Y, Wang J-C et al (1992) Design and geometry of face-gear drives. J Mech Des 114:642–647. https://doi.org/10.1115/1.2917055
4. Tang J, Yin F, Chen X (2013) The principle of profile modified face-gear grinding based on disk wheel. Mech Mach Theory 70:1–15. https://doi.org/10.1016/j.mechmachtheory.2013.06.013
5. Tang J, Cui W, Zhou H, Yin F (2016) Integrity of grinding face-gear with worm wheel. J Cent South Univ 23:77–85. https://doi.org/10.1007/s11771-016-3051-y
6. Zhou R, Zhao N, Li W et al (2019) A grinding method of face gear mating with a conical spur involute pinion. Mech Mach Theory 141:226–244. https://doi.org/10.1016/j.mechmachtheory.2019.07.013
7. Wang Y, Hou L, Lan Z, Zhang G (2016) Precision grinding technology for complex surface of aero face-gear. Int J Adv Manuf Technol 86:1263–1272. https://doi.org/10.1007/s00170-015-8241-5
8. Litvin FL, Gonzalez-Perez I, Fuentes A et al (2005) Design, generation and stress analysis of face-gear drive with helical pinion. Comput Methods Appl Mech Eng 194:3870–3901. https://doi.org/10.1016/j.cma.2004.09.006
9. Li G, Ran Q, He K, et al (2023) Forming dressing method of the crown worm wheel based on virtual center distance principle. Comput Integr Manuf Syst 29:3394–3401. https://kns.cnki.net/kcms/detail/11.5946.TP.20210823.1001.006.html
10. He K, He X, Li G et al (2023) The continuous generating grinding method for face gears based on general cylindrical gear grinding machine. Int J Adv Manuf Technol 125:4133–4147. https://doi.org/10.1007/s00170-023-10983-4
11. Shi X, Zhou Y, Tang J, Li Z (2020) An innovative generated approach to dressing the worm for grinding spur face gears. Manufacturing Letters 25:26–29. https://doi.org/10.1016/j.mfglet.2020.06.003
12. Zhou Y, Tang Z, Shi X et al (2022) Efficient and accurate worm grinding of spur face gears according to an advanced geometrical analysis and a closed-loop manufacturing process. J Cent South Univ 29:1–13. https://doi.org/10.1007/s11771-021-4830-7
13. Huang W, Tang J, Zhou W et al (2023) Molecular dynamics simulations of ultrasonic vibration-assisted grinding of polycrystalline iron: nanoscale plastic deformation mechanism and microstructural evolution. Appl Surf Sci 640:158440. https://doi.org/10.1016/j.apsusc.2023.158440
14. Zhou W, Tang J, Li Z et al (2023) Study on scratch hardness in ultrasonic vibration-assisted scratching based on instantaneous

contact analysis. Wear 528–529:204991. https://doi.org/10.1016/j.wear.2023.204991

15. Zhou W, Tang J, Shao W, Wen J (2022) Towards understanding the ploughing friction mechanism in ultrasonic assisted grinding with single grain. Int J Mech Sci 222:107248. https://doi.org/10.1016/j.ijmecsci.2022.107248

16. Shi X, Zhou Y, Zhang W, Tang J (2019) A new worm grinding method of face gears based on the optimization of dressing wheel profile. Forsch Ingenieurwes 83:751–757. https://doi.org/10.1007/s10010-019-00353-6

17. Shen Y, Liu X, Li D, Li Z (2018) A method for grinding face gear of double crowned tooth geometry on a multi-axis CNC machine. Mech Mach Theory 121:460–474. https://doi.org/10.1016/j.mechmachtheory.2017.11.007

18. Guo H, Zhang S, Wu T, Zhao N (2021) An approximate design method of grinding worm with variable meshing angle and grinding experiments of face gear. Mech Mach Theory 166:104461. https://doi.org/10.1016/j.mechmachtheory.2021.104461

19. Peng X, Zhou J (2022) Optimization design for dynamic characteristics of face gear drive with surface-active modification. Mech Mach Theory 176:105007. https://doi.org/10.1016/j.mechmachtheory.2022.105007